

CREEP MODELLING IN A COMPOSITE ROTATING DISC WITH THICKNESS VARIATION IN THE PRESENCE OF RESIDUAL STRESS

MODELIRANJE PUZANJA KOD ROTIRAJUĆEG DISKA PROMENLJIVE DEBLJINE OD KOMPOZITA U PRISUSTVU ZAOSTALIH NAPONA

Originalni naučni rad / Original scientific paper
UDK /UDC: 539.3/4:519.87
Rad primljen / Paper received: 06.06.2016.

Adresa autora / Author's address:

¹Punjabi University Patiala, Department of Mathematics, Punjab, India

²ICFAI University, Faculty of Science and Technology, Dept. of Mathematics, Solan, Himachal Pradesh, India, pankaj_thakur15@yahoo.co.in

Keywords

- creep
- rotating disc
- residual stress
- composites

Abstract

In the presence of residual stress in an isotropic / anisotropic disc, the nature of radial strain rate changes from compressive to tensile, particularly in the middle region of the disc with linear thickness as compared to the disc without residual stresses. Further, the magnitude of residual stress effect in the anisotropic disc is significantly lower as compared to those for the isotropic disc. For designing a rotating disc with linear thickness operating at elevated temperature, the presence of residual stress needs attention from the point of view of steady state creep rate. Although, the effect of residual stress on the steady state creep rate in the anisotropic disc is observed to be significantly lower than that observed in the isotropic disc.

INTRODUCTION

Residual stresses significantly affect the engineering properties of materials and structural components, notably fatigue life, distortion, dimensional, corrosion resistance, brittle fracture etc. For that reason, the residual stress analysis is an important stage in the design of parts and structural elements. Residual stresses in a structural material are the system of stresses which exist in a body in the absence of external loads. Residual stresses can be present in any mechanical structure because of processing used to make the composite material. However, processing of the composite material often involves cooling from higher temperature resulting in thermal residual stresses in the matrix due to restraint imposed by ceramic reinforcements. Residual stresses are to be considered as only elastic stresses. The maximum value that a residual stress can reach is the elastic limit of the material. A stress in excess of this value, with no external force to oppose it, will relieve itself by plastic deformation until it reaches the value of the yield stress.

The thermal residual stresses induced due to thermal mismatch between the metal matrix and the ceramic reinforcement in metal matrix composite may impart plastic deformation to the matrix. Thermal mismatch strains also

Ključne reči

- puzanje
- rotirajući disk
- zaostali naponi
- kompoziti

Izvod

U prisustvu zaostalog napona kod izotropnog / anizotropnog diska, priroda brzine promene radijalnih deformacija se menja od pritisnih pa do zateznih, posebno u središnjem delu diska linearne promenljive debljine, u poređenju sa diskom bez zaostalih napona. Osim toga, uticaj zaostalih napona kod anizotropnog diska je značajno manji u poređenju sa izotropnim diskom. Prisustvo zaostalih napona u proračunu rotirajućeg diska sa linearnom primenljivom debljinom za rad na povišenoj temperaturi zahteva posebnu pažnju s obzirom na brzinu ravnomernog puzanja. Premda je kod anizotropnog diska uticaj zaostalih napona na brzinu ravnomernog puzanja znatno manji u odnosu na slučaj kod izotropnog diska.

may quite often crack the matrix resulting in a relaxation of the residual stresses. Presence of thermal residual stresses can induce the asymmetry in the tensile and compressive yield stresses of the composite. Residual stresses may be reduced or eliminated by annealing, plastic deformation or just by letting the piece at room temperature enough time. Because of its influence on the properties, the residual stress in composites has been the subject of several studies, both experimental and analytical (Arsenault and Taya 1987, Jahed and Dubey 1997, Singh and Ray 2003, 2004, Singh and Rattan 2010). Badini (1990) studied the correlation between the microstructure and the tensile and compressive properties of composite extruded bars of 6061 Al alloy matrix reinforced with silicon carbide whiskers. The compressive strength in the longitudinal direction was considerably higher than the strength in the transverse direction. Compressive and tensile strengths of cylindrical samples, having 20 mm diameter, were found to be 218 MPa and 186 MPa, respectively. Further, the mechanical strength of the material was observed to depend on the loading direction, due to orientation of whiskers that contribute to reinforcing the composite to different degrees depending on their alignment in the direction of load applied.

Jahed and Shirazi (2001) investigated loading and residual stresses, and associated strains and displacements in a thermoplastic rotating variable thickness disc at elevated temperatures by using variable material properties (VMP) method in which any yield criterion (i.e. von Mises or Tresca) and any hardening rule (i.e. isotropic or kinematic) for characterization of uploading may be used.

Carrera et. al. (2007) described the procedure followed to measure the residual stresses that develop in the critical region of cast engine blocks made from a heat treatable aluminium silicon copper alloy. The measurement in automotive engine blocks with cast-in grey iron liners indicated the development of tensile stresses higher than 150 MPa, depending on the geometry and size of the piece. It was considered that such stresses originated during cooling of the aluminium alloy restricted by iron liners. In other words, residual stresses were the differences in the thermal expansion coefficient of iron and aluminium and, if high enough, may promote the failure of the block. Such observation was confirmed by measurements carried out in engine blocks cast without liners that develop compressive stresses of around -20 MPa in their cylinder bridges.

Keeping in view, because of the significant practical importance of the thermal residual stress, the objective of the present study has been to investigate the effects of thermal residual stress on stress distributions and the resulting creep deformation of the rotating disc made of silicon carbide particulate reinforced aluminium base composite. The analysis has been done for isotropic/anisotropic composite discs of linearly varying thickness in the presence/absence of thermal residual stresses by using isotropic/anisotropic Hoffman yield criterion. Results have been compared with those obtained using von Mises yield/ Hill's criterion ignoring difference in yield stresses. The creep behaviour of the composite disc rotating at 15 000 rpm has been described by Sherby's constitutive model. The creep response of rotating disc is expressed by a threshold stress with value of stress exponent as 8. The material parameters characterizing difference in yield stresses have been used from the available experimental results in literature. Stress and strain rate distributions developed due to rotation have been calculated.

It is concluded that the presence of thermal residual stresses in composite rotating disc with linearly varying thickness needs attention for designing a disc.

ANALYSIS OF CREEP IN A DISC OF VARIABLE THICKNESS

Consider the particle reinforced composite disc of density ρ and with variable thickness h , rotating with constant angular speed ω radian/s, and let a and b be inner and outer radii of the disc, respectively. Let I and I_0 denote the moment of inertia of the disc at inner radius $r = a$ and outer radius $r = b$, respectively as shown in Fig. 1. A and A_0 denote the area of cross section of disc at inner a and outer radius b , respectively. Then,

$$I = \int_a^r hr^2 dr, I_0 = \int_a^b hr^2 dr, A = \int_a^r h dr, A_0 = \int_a^b h dr \quad (1)$$

where, the average tangential stress may be defined as

$$\sigma_{\theta avg} = \frac{1}{A_0} \int_a^b h \sigma_{\theta} dr \quad (2)$$

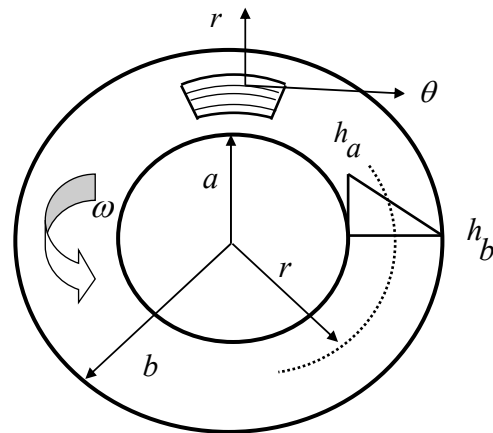


Figure 1. A rotating disc with linear thickness.

For the purpose of creep analysis in disc with variable thickness, the following assumptions are made:

1. Material of disc is orthotropic and incompressible.
2. Elastic deformations are small for the disc and therefore they can be neglected as compared to creep deformation.
3. Axial stress in the disc may be assumed to be zero as thickness of disc is assumed to be very small compared to its diameter.
4. The composite shows a steady state creep behaviour, which may be described by following Sherby's constitutive model (1977) of the form,

$$\dot{\epsilon} = A_s \left(\frac{\bar{\sigma} - \sigma_0}{E} \right)^n,$$

where: $A_s = \frac{AD_\lambda \lambda^3}{|b_r|^5}$, and $\dot{\epsilon}, \bar{\sigma}, n, \sigma_0, A, D_\lambda, \lambda, b_r, E$

are the effective strain rate, effective stress, the stress exponent, threshold stress, a constant, lattice diffusivity, the sub-grain size, the magnitude of burgers vector, and Young's modulus, in respect.

The above equation may be expressed as:

$$\dot{\epsilon} = [M(\bar{\sigma} - \sigma_0)]^n \quad (3)$$

where: $M = \frac{A_s^{1/n}}{E}$ is the creep parameter.

The different material combinations in the composite are conceptually replaced by an equivalent monolithic material that has the yielding and creep behaviour similar to those displayed by the composite. Taking reference frame along the principal directions of r, θ and z , the generalized constitutive equations for an anisotropic disc under multiaxial stress condition are given as:

$$\dot{\epsilon}_r = \frac{\dot{\epsilon}}{2\bar{\sigma}} \{ (G + H)\sigma_r - H\sigma_\theta - G\sigma_z + (f_c - f_t) \} \quad (4)$$

$$\dot{\varepsilon}_\theta = \frac{\dot{\bar{\varepsilon}}}{2\bar{\sigma}} \{ (H+F)\sigma_\theta - F\sigma_z - H\sigma_r + (f_c - f_t) \} \quad (5)$$

$$\dot{\varepsilon}_z = \frac{\dot{\bar{\varepsilon}}}{2\bar{\sigma}} \{ (F+G)\sigma_z - G\sigma_r - F\sigma_\theta + (f_c - f_t) \} \quad (6)$$

where the effective stress, $\bar{\sigma}$, is given by

$$\bar{\sigma} = \left\{ \frac{1}{(G+H)} \left[F(\sigma_\theta - \sigma_z)^2 + G(\sigma_z - \sigma_r)^2 + H(\sigma_r - \sigma_\theta)^2 \right] \right\}^{1/2}$$

where F , G and H are anisotropic constants of the material. $\dot{\varepsilon}_r$, $\dot{\varepsilon}_\theta$, $\dot{\varepsilon}_z$ and σ_r , σ_θ , σ_z are the strain rates and the stresses respectively in the direction r , θ and z . $\dot{\bar{\varepsilon}}$ is the effective strain rate and $\bar{\sigma}$ is the effective stress and f_c , f_t are uniaxial compression- and tensile yield stresses, in respect. For biaxial state of stress (σ_r , σ_θ), the effective stress is

$$\bar{\sigma} = \left\{ \frac{1}{(G+H)} \left[F\sigma_\theta^2 + G\sigma_r^2 + H(\sigma_r - \sigma_\theta)^2 \right] \right\}^{1/2} \quad (7)$$

Using Eqs.(3) and (7), Eq.(4) can be rewritten as

$$\dot{\varepsilon}_r = \frac{d\dot{u}_r}{dr} = \frac{\left[\left(\frac{G}{F} + \frac{H}{F} \right) x - \frac{H}{F} + \frac{f_c - f_t}{\sigma_\theta} \right] [M(\bar{\sigma} - \sigma_0)]^8}{\sqrt{\frac{G}{F} + \frac{H}{F}} \left[\left(\frac{G}{F} + \frac{H}{F} \right) x^2 - 2\frac{H}{F}x + \left(\frac{G}{F} + \frac{H}{F} \right) \right]^{1/2}} \quad (8)$$

Similarly from Eq.(5),

$$\dot{\varepsilon}_\theta = \frac{\dot{u}_r}{r} = \frac{\left[\left(1 + \frac{H}{F} \right) - \frac{H}{F}x + \frac{f_c - f_t}{\sigma_\theta} \right] [M(\bar{\sigma} - \sigma_0)]^8}{\sqrt{\frac{G}{F} + \frac{H}{F}} \left[\left(\frac{H}{F} + \frac{G}{F} \right) x^2 - 2\frac{H}{F}x + \left(1 + \frac{H}{F} \right) \right]^{1/2}} \quad (9)$$

From the material's incompressibility assumption, it follows that

$$\dot{\varepsilon}_z = -(\dot{\varepsilon}_r + \dot{\varepsilon}_\theta) \quad (10)$$

where: $x = \frac{\sigma_r}{\sigma_\theta}$ is the ratio of radial and tangential stresses,

and $\dot{u}_r = du/dt$ is the radial deformation rate.

Dividing Eq.(1) by Eq.(2),

$$\varphi(r) = \frac{[(G/F) + (H/F)]x - (H/F) + [(f_c - f_t)/\sigma_\theta]}{[1 + (H/F)] - (H/F)x + [(f_c - f_t)/\sigma_\theta]} \quad (11)$$

where: $\varphi(r) = \frac{d\dot{u}_r}{dr} \cdot \frac{r}{\dot{u}_r}$. This implies $\frac{d\dot{u}_r}{\dot{u}_r} = \frac{\varphi(r)}{r} dr$.

Integrating and taking limit a to r on both sides,

$$\dot{u}_r = \dot{u}_i \exp \int_a^r \frac{\varphi(r)}{r} dr \quad (12)$$

where: \dot{u}_i is the radial deformation rate at the inner radius.

Dividing Eq.(12) by r and equating to Eq.(2),

$$\bar{\sigma} - \sigma_0 = \frac{(\dot{u}_i)^{1/8}}{M} \psi(r) \quad (13)$$

where:

$$\psi(r) = \left\{ \frac{\sqrt{\frac{G}{F} + \frac{H}{F}} \left[\left(\frac{H}{F} + \frac{G}{F} \right) x^2 - 2\frac{H}{F}x + \left(1 + \frac{H}{F} \right) \right]^{1/2}}{r \left[\left(1 + \frac{H}{F} \right) - \frac{H}{F}x + \frac{f_c - f_t}{\sigma_\theta} \right]} \exp \int_a^r \frac{\varphi(r)}{r} dr \right\}^{1/8} \quad (14)$$

Substituting $\bar{\sigma}$ from Eq.(7) into Eq.(13), it gives

$$\left\{ \left(\frac{F}{G+F} \right) \left[\left(\frac{G}{F} + \frac{H}{F} \right) x^2 - 2\frac{H}{F}x + \left(\frac{H}{F} + 1 \right) \right] \right\}^{1/2} \sigma_\theta - \sigma_0 = \frac{(\dot{u}_i)^{1/8}}{M} \psi(r)$$

This implies

$$\sigma_\theta = \frac{(\dot{u}_i)^{1/8}}{M} \psi_1(r) + \psi_2(r) \quad (15)$$

where:

$$\psi_1(r) = \frac{\psi(r)}{\left\{ \left(\frac{F}{G+H} \right) \left[\left(\frac{G}{F} + \frac{H}{F} \right) x^2 - 2\frac{H}{F}x + \left(1 + \frac{H}{F} \right) \right] \right\}^{1/2}} \quad (16)$$

and

$$\psi_2(r) = \frac{\sigma_0}{\left\{ \left(\frac{F}{G+H} \right) \left[\left(\frac{G}{F} + \frac{H}{F} \right) x^2 - 2\frac{H}{F}x + \left(1 + \frac{H}{F} \right) \right] \right\}^{1/2}} \quad (17)$$

The equation of equilibrium for a rotating disc with varying thickness can be written as:

$$\frac{d}{dr} (rh\sigma_r) - h\sigma_\theta + \rho\omega^2 r^2 h = 0 \quad (18)$$

Integrating Eq.(18) within limits a to b and using Eq.(1) and Eq.(2),

$$\sigma_{\theta_{avg}} = \frac{1}{A_0} \rho\omega^2 I_0 \quad (19)$$

Substituting σ_θ from Eq.(15) into Eq.(2),

$$\frac{(\dot{u}_i)^{1/8}}{M} = \frac{A_0 \sigma_{\theta_{avg}} - \int_a^b \psi_2(r) h dr}{\int_a^b \psi_1(r) h dr} \quad (20)$$

Using Eq.(19) and Eq.(20), Eq.(15) becomes,

$$\sigma_\theta = \frac{\psi_1(r) \left[\rho\omega^2 I_0 - \int_a^b \psi_2(r) h dr \right]}{\int_a^b \psi_1(r) h dr} + \psi_2(r) \quad (21)$$

Integrating Eq.(18) within limits a to r and using Eq.(1),

$$\sigma_r = \frac{1}{rh} \left[\int_a^r \sigma_\theta h dr - \rho\omega^2 I \right] \quad (22)$$

Thus, the tangential stress σ_θ and the radial stress σ_r are determined by Eqs.(21) and (22). Then strain rates $\dot{\varepsilon}_r$, $\dot{\varepsilon}_\theta$ and $\dot{\varepsilon}_z$ calculated from Eqs.(5), (6) and (7).

NUMERICAL COMPUTATIONS

The stress distribution and strain rates are evaluated for the rotating discs having linearly varying thickness by iterative numerical scheme of computations depicted in Fig. 2.

In the first iteration, it is assumed that $\sigma_\theta = \sigma_{avg}$ over the entire disc radii. Substituting σ_{avg} for σ_θ in Eq.(22), the first approximation value of σ_r i.e. $[\sigma_r]_1$ is obtained. The first approximation of stress ratio i.e. $[x]_1$, is obtained by dividing $[\sigma_r]_1$ by σ_θ which can be substituted in Eq.(11) to calculate the first approximation of $\psi(r)$ i.e. $[\psi(r)]_1$. Now one carries out the numerical integration of $[\phi(r)]_1$ from limits of a to r and uses this value in Eq.(14) to obtain first

approximation of $\psi(r)$ i.e. $[\psi(r)]_1$. Using this $[\psi(r)]_1$ and σ_θ in Eqs.(16) and (17) respectively, $[\psi_1(r)]_1$ and $[\psi_2(r)]_1$ are found, which are used in Eq.(15) to find second approximation of σ_θ i.e. $[\sigma_\theta]_2$. Using $[\sigma_\theta]_2$ for σ_θ in Eq.(22), the second approximation of σ_r i.e. $[\sigma_r]_2$ is found and then the second approximation of x i.e. $[x]_2$ is obtained. The iteration is continued till the process converges and gives the values of stresses at different points of the radius grid. For rapid convergence 75 percent of the value of σ_θ obtained in the current iteration has been mixed with 25 percent of the value of σ_θ obtained in the last iteration for use in the next iteration i.e. $\sigma_{\theta next} = 0.25 \cdot \sigma_{\theta previous} + 0.75 \cdot \sigma_{\theta current}$.

LEGENDS:

ITER = Iteration no

h = Limiting value of Err (=0.01)

ITM = Maximum no of iterations

$$ERR = \frac{[\sigma_\theta(r)]_{ITER} - [\sigma_\theta(r)]_{ITER-1}}{[\sigma_\theta(r)]_{ITER-1}}$$

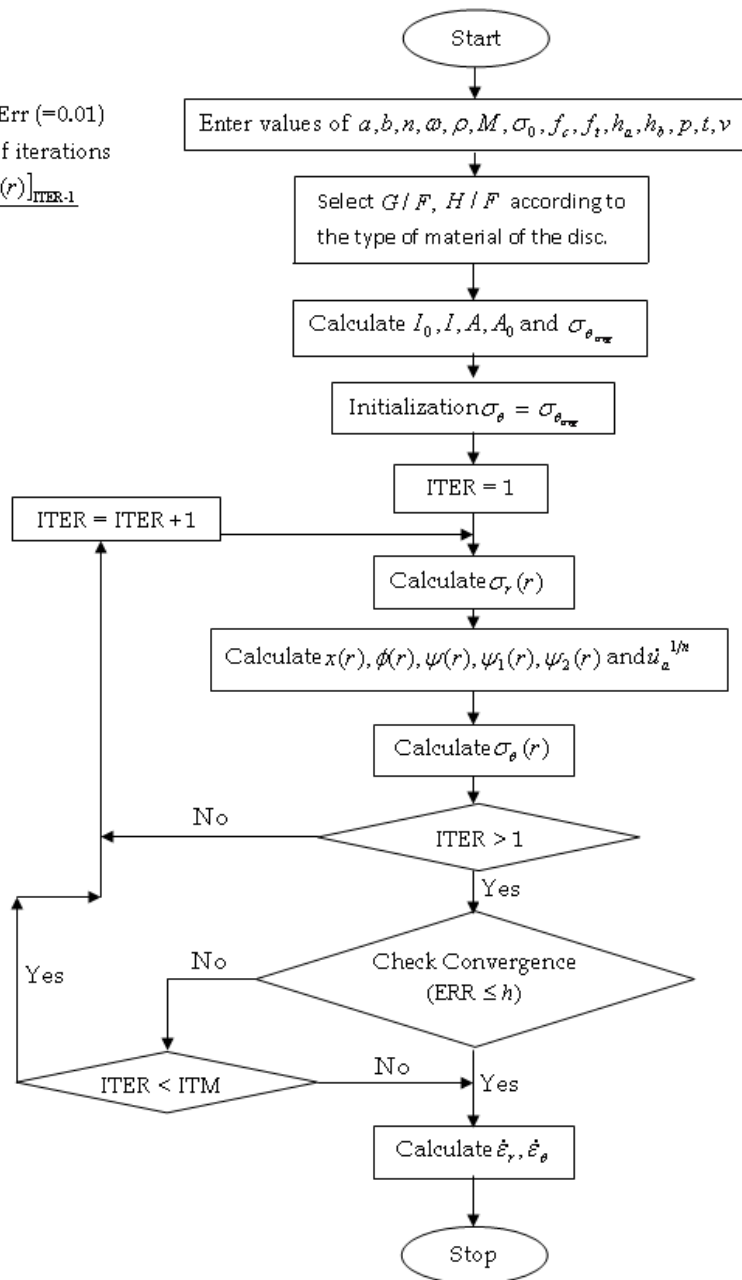


Figure 2. Numerical scheme of computations.

RESULTS AND DISCUSSION

A computer program based on the analysis presented has been developed to obtain the stress distributions and strain rate of the rotating varying thickness discs containing silicon carbide particle in a matrix of pure aluminium in the presence of thermal residual stress, and the obtained results are compared to the disc without residual stresses so to analyse the importance of the residual stress. The parameters used here for the analysis are given in Table 1. The analysis is carried out and the developed computer programme is validated by following the described procedure. Once again, a good agreement is noticed between the results obtained from the current investigation and those obtained experimentally by Wahl et al. (1954). For the analysis, the tensile residual stress ($\Delta\sigma_y$) is taken as 32 MPa (used by Badini 1990, Singh and Rattan 2010).

For an anisotropic disc with linearly varying thickness, the disc thickness at the inner and outer radii are obtained respectively as $h_a = 1.44$ mm and $h_b = 0.75$ mm, while for the anisotropic disc with hyperbolically varying thickness, the thickness at the inner and outer radii are obtained respectively as $h_a = 2.42$ mm and $h_b = 0.76$ mm. The creep analysis in a rotating disc of Al-SiC (particle) composite having linearly varying thickness, shown in Fig. 1, is carried using isotropic/anisotropic Hoffman yield criterion of yielding and results are compared with those using the von Mises yield criterion / Hill's criterion of yielding, ignoring the difference in yield stresses, i.e. ($\Delta\sigma_y = 0$).

Figure 3 shows the tangential stress in an isotropic/anisotropic rotating disc with linearly varying thickness in the

Table 1. Parameters and operating conditions for the steel disc.

Parameters of steel disc	
Density of disc material	$\rho = 2812.4 \text{ kg/m}^3$
Inner radius of disc	$a = 31.75 \text{ mm}$
Outer radius of disc	$b = 152.4 \text{ mm}$
Particle size	$P = 1.7 \text{ }\mu\text{m}$
Particle content	$V = 20\%$
Creep parameters	$M = 5.83 \times 10^{-3} \text{ s}^{-1/8}/\text{MPa}$ and $\sigma_0 = 24.44 \text{ MPa}$
Young's modulus	$E(\text{Al})=70 \text{ GPa}, E(\text{SiC})=47 \text{ GPa}$
Density	$\rho(\text{Al}) = 2713 \text{ kg/m}^3,$ $\rho(\text{SiC}) = 3210 \text{ kg/m}^3$
The stress exponent of disc	$n = 8$
The ratio of anisotropic constants	$G/F = 1.34, H/F = 1.64$
The ratio of isotropic constants	$G/F = 1, H/F = 1$
Operating conditions	
Angular velocity of Disc	$\omega = 15 \text{ 000 rpm}$
Operating temperature	$T = 616 \text{ K}$
Creep duration	$t = 180 \text{ hrs.}$

presence of residual stresses and the results are compared to those without residual stress. It is concluded that in isotropic/anisotropic discs, the tangential stress is a little lower in the region near the inner radius and slightly higher in the region near to the outer radius in the presence of residual stress, as compared to the disc without residual stress. It is also noted that the effect of residual stress on the tangential stress distribution is lesser in an anisotropic rotating disc of linearly varying thickness compared to an isotropic disc of linearly varying thickness. Also the tangential stress becomes more uniform in the presence/absence of residual stress in an anisotropic disc compared to an isotropic disc.

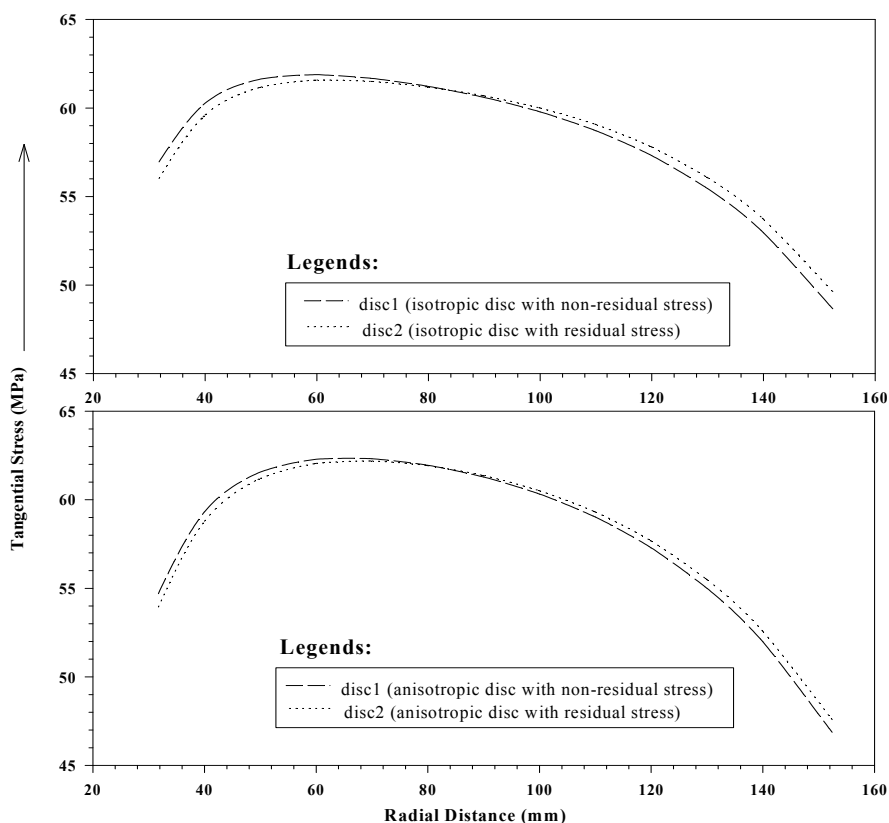


Figure 3. Variation of tangential stress along the radial distance in isotropic/anisotropic discs rotating 15000 rpm at 616 K.

Figure 4 shows the variation of radial stresses along the radius of the isotropic/anisotropic rotating disc in the presence/absence of residual stress. It is observed that in the presence of residual stress, the radial stress developing due to rotation is slightly lesser than the radial stress of an isotropic/anisotropic disc without residual stress, although the change in the magnitude of radial stress distribution is very small in isotropic/anisotropic discs with linear thickness due to the presence of residual stresses. As one moves from the inner to the outer radius of the disc, the radial stress increases from zero and reaches a maximum near the middle region of the disc with linear thickness and then starts decreasing towards the outer region.

Figure 5 shows that in the presence of tensile residual stress, the tangential strain rates enhance significantly in both the isotropic/anisotropic discs compared to the discs without residual stress. Also, the difference in the tangential strain rate caused due to the presence and the absence of residual stresses (i.e. the residual effect) goes on increasing with radial distance and the extent of the increased difference is maximum in the region near the outer radius in both the isotropic/anisotropic discs having linearly varying thickness. Secondly, it is also noticed that variation in magnitude due to residual stress in an anisotropic disc is smaller compared to that for an isotropic disc. In an isotropic/anisotropic disc with/without residual stress, the tangential strain rates are highest at the inner radius and

then decrease continuously, when one moves towards the outer radius of the disc. The trend of variation of tensile strain rate in the tangential direction remains the same in an isotropic/anisotropic disc in the presence/absence of residual stresses, but the magnitude can be reduced in an anisotropic disc.

Figure 6 shows, in the presence of residual stresses, the radial strain rate in an isotropic/anisotropic rotating disc with linear thickness, and the results are compared to those without residual stress. From both discs of isotropic/anisotropic material, it is concluded that in the absence of residual stress, the nature of the radial strain rate which is compressive, becomes tensile at the middle of the disc in the presence of residual stress. It is also noticed that the difference in strain rate caused due to the presence and absence of residual stresses is smaller in an anisotropic disc as compared to that for an isotropic disc. Another point to be observed is that the magnitude of radial strain rate firstly increases rapidly with radial distance and then starts to decrease. It reaches a minimum before increasing again towards the outer radius in both the isotropic/anisotropic discs with residual/without residual stress.

From the above discussion, it can be concluded that residual stresses may cause significant distortion in an isotropic/anisotropic rotating disc having linearly varying thickness, but the magnitude of distortion can be reduced by selecting anisotropic disc.

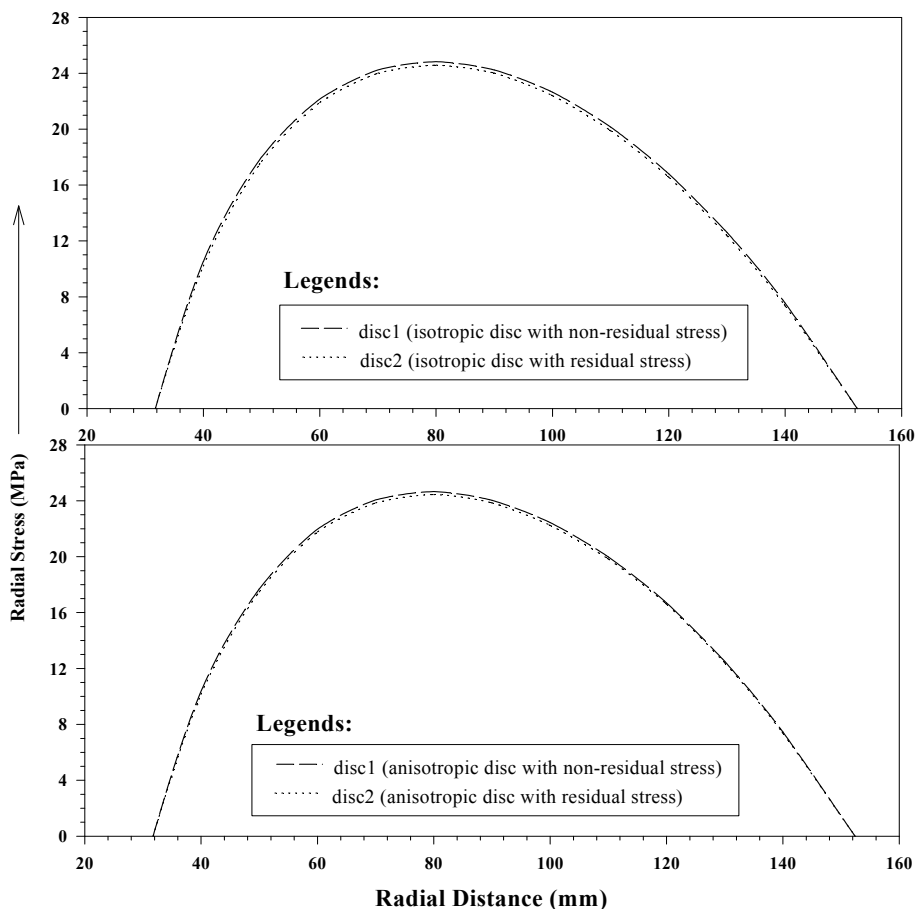


Figure 4. Variation of radial stress along the radial distance in isotropic/anisotropic discs rotating 15000 rpm at 616 K.

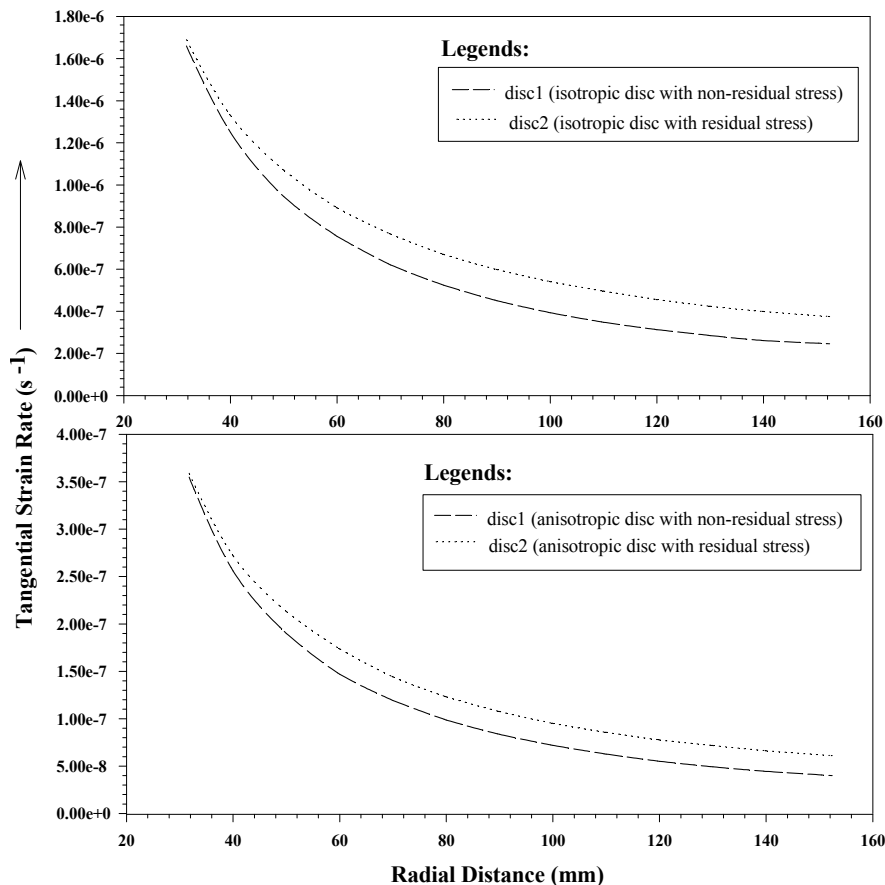


Figure 5. Variation of tangential strain rate along the radial distance in isotropic/anisotropic discs rotating 15000 rpm at 616 K.

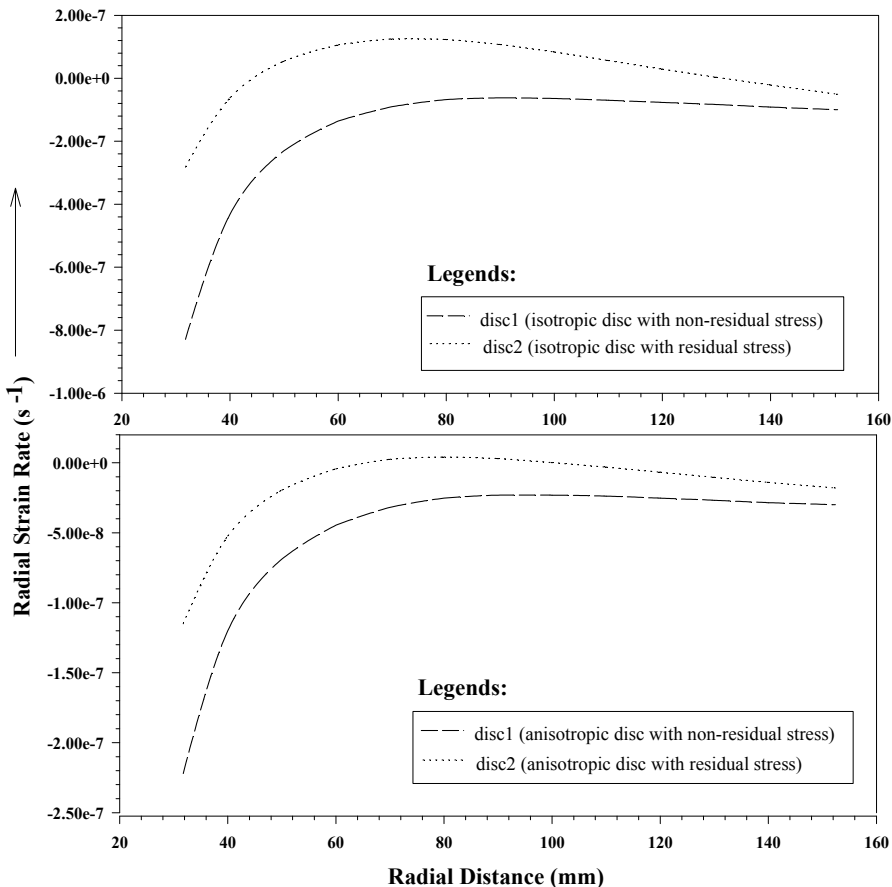


Figure 6. Variation of radial strain rate along the radial distance in isotropic/anisotropic discs rotating 15000 rpm at 616 K.

CONCLUSIONS

The above results and discussion lead to conclusions:

1. The presence of the thermal residual stress developing due to rotation does not significantly affect the distribution of stress in the isotropic/anisotropic disc having linearly varying thickness, but it affects the strain rates significantly.
2. The magnitude of variation of tangential stress and the radial stress obtained in the anisotropic disc with/without residual stress are relatively smaller as compared to that for the isotropic rotating disc.
3. In the isotropic/anisotropic disc, the tangential strain rate is more in presence of thermal residual stress. Also, the extent of difference in creep caused due to the presence/absence of the residual stress increases as one moves towards the outer radius of the disc, although the magnitude of this difference is smaller in an anisotropic disc compared to the isotropic disc.
4. In the presence of residual stresses in the isotropic/anisotropic disc, the nature of radial strain rate changes from compressive to tensile, particularly in the middle region of the disc with linear thickness, as compared to the disc without residual stresses. Further, the magnitude of residual stress effect in the anisotropic disc is significantly lower as compared to those for the isotropic disc.
5. For designing a rotating disc with linear thickness, operating at elevated temperature, the presence of residual stress needs attention from the point of view of steady state creep rate. Although, the effect of residual stress on the steady state creep rate in the anisotropic disc is observed to be significantly lower than that observed in the isotropic disc.

ECF 22 ANNOUNCEMENT

The Society for Structural Integrity and Life (DIVK) will organise the 22nd European Conference of Fracture (ECF22) in Belgrade. The venue of the conference is the University of Belgrade, Faculty of Mechanical Engineering and Faculty of Technology and Metallurgy.

Topic: Loading and Environmental Effects on Structural Integrity

The topics at the ECF 22 should be focused on experienced, possible and predictable fracture and failures, considering inter-relation between external effects (loading, environment), structure characteristics, components strength and material properties.

Safety and reliability problems during operation life, including maintenance and repair, represent also items, very important for structural integrity. Specifically, applied stress-strain state in critical structural components, induced by acting loading at global level, and affected by stress concentration at the local level should be considered theoretically and applying convenient numerical modelling.

In addition to structures of macro to micro scales of commonly used metallic and non-metallic materials, attention will be paid to the new huge complex structures of civil engineering objects, well exceeding classical objects of macro size on one side, and structures of nano level on the other side. Structural integrity, functionality, reliability and safety of such structures and applied materials require special consideration.

REFERENCES

1. Arsenault, R.J., Taya, M. (1987), *Thermal residual stress in metal matrix composite*, Acta Metallurgica, 35(3): 651-659.
2. Badini, C. (1990), *SiC Whiskers-aluminum 6061 composite: microstructure and mechanical characteristic anisotrop*, J Mat. Sci., 25: 2607-2614.
3. Carrera, E., Rodriguez, A., Talarnantes, J., Valtierra, S., Colas, R. (2007), *Measurement of residual stresses in cast aluminum engine blocks*, J Mater. Proc. Techn., 189: 206-210.
4. Jahed, H., Dubey, R. N. (2014), *An axisymmetric method of elastic-plastic analysis capable of predicting residual stress field*, Intern. J Fatigue 64: 33-41.
5. Gupta, S.K., Pankaj, T. (2007), *Thermo elastic-plastic transition in a thin rotating disc with inclusion*, Thermal Science, 11 (1): 103-118.
6. Jahed, H., Shirazi, R. (2001), *Loading and unloading behaviour of a thermoplastic disc*, Intern. J Pressure Ves. and Piping 78(9): 637-645.
7. Rattan, M., Chamoli, N., Singh, S.B. (2010), *Creep analysis of an isotropic functionally graded rotating disc*, Int. J Contemp. Math. Sciences 5(9): 419-431.
8. Singh, S.B., Ray, S. (2003), *Newly proposed yield criterion for residual stress and steady state creep in an anisotropic composite rotating disc*, J Mater. Proc. and Techn. 143-144: 623-628.
9. Singh, S.B., Ray, S. (2004), *Modeling the creep in an isotropic rotating disc of Al-SiC composite in presence of thermal residual stress*, Proc. 3rd Int. Conf. on Advanced Manufact. Techn.: ICAMT-2004, May 11-13, Kuala Lumpur, Malaysia, 766-770.
10. Wahl, A.M., Sankey, G.O., Manjoine, M.J., Shoemaker, E. (1954), *Creep tests of rotating disks at elevated temperature and comparison with theory*, J App. Mech. 76: 225-235.

Loading types

static and quasi-static loading; cyclic loading of variable amplitudes (high cycle-loading well below yield stress; low cycle loading after initial yielding); vibrations; impact and earthquake loading; combined loading

Environment

corrosion; stress corrosion; high operating temperatures; temperatures in the range of nil ductility transition (NDT) and below it; combined environmental effects

Structures

thermo electrical power; hydro electrical power plants; nuclear power plants; process equipment and plants in petrochemical industry; welded structures; civil engineering objects; transportation means

Materials

Steel; metallic materials; plastics; nonmetallic materials; composite materials; nano materials; bio-materials

Proceedings and Publications

Two-page abstracts will be published in the form of ECF22 Proceedings Book. CD-ROM will be available during registration. Also on the ESIS website. Selected papers shall be published as special issues of 'Engineering Fracture Mechanics', 'Engineering Failure Analysis' or 'International Journal of Fatigue'.

